

TO: AIRS Design File**DATE:** 12 June 2002**FROM:** Mark Hofstadter**SUBJECT:** Vis/NIR On-Orbit Checkout**KEYWORDS:** Vis/NIR, Calibration, Lamp, Geolocation, Detector Numbering

ABSTRACT: This report presents an initial assessment of the on-orbit performance of the Vis/NIR system. Noise levels are in excellent agreement with pre-launch testing. Calibration lamp performance is close, but not identical to expected patterns. There is also a hint of a low-level signal in parts of the blackbody field. Neither of these unexpected results are considered serious at this time. Co-registration of the four Vis/NIR channels and the absolute geolocation of data products look excellent: no errors can be found at a resolution of 0.18 degrees (~2 km at nadir). As an aside, the convention for detector numbering is also discussed. The next phase of Vis/NIR checkout will focus on vicarious radiometric calibration and cloud detection over ocean.

Introduction

The Aqua spacecraft launched in the early morning of 4 May 2002, and high-rate data from the AIRS instrument began late on 16 May. Between the 16th and the 26th, when the scan mirror started rotating, valid dark-current readings on all Vis/NIR detectors were collected while staring into the blackbody cavity. At 01:06 UTC on 26 May 2002 (18:06 PDT of 25 May 2002) the AIRS scan mirror started, and valid scene data was received. First-light images, primarily for public relations purposes, were collected in a brief report and placed on the internal AIRS web-page (<http://airsteam.jpl.nasa.gov>).

This document summarizes the first assessments of instrument performance: dark current and noise levels (including response to the South Atlantic Anomaly), calibration lamp signal levels and short-term stability, co-registration of the Vis/NIR channels, and absolute geolocation accuracy of the Vis/NIR products. The instrument and software, as well as the overall data flow from the spacecraft to JPL, appear to be in excellent shape. All aspects of the current analysis will be revisited over the coming months to refine the results and look at longer term trends. As per plan, however, the next phases of checkout will focus on vicarious radiometric calibration and the Vis/NIR cloud flag over ocean.

(As an aside, an important clarification on the detector numbering convention can be found in the footnote on page 11.)

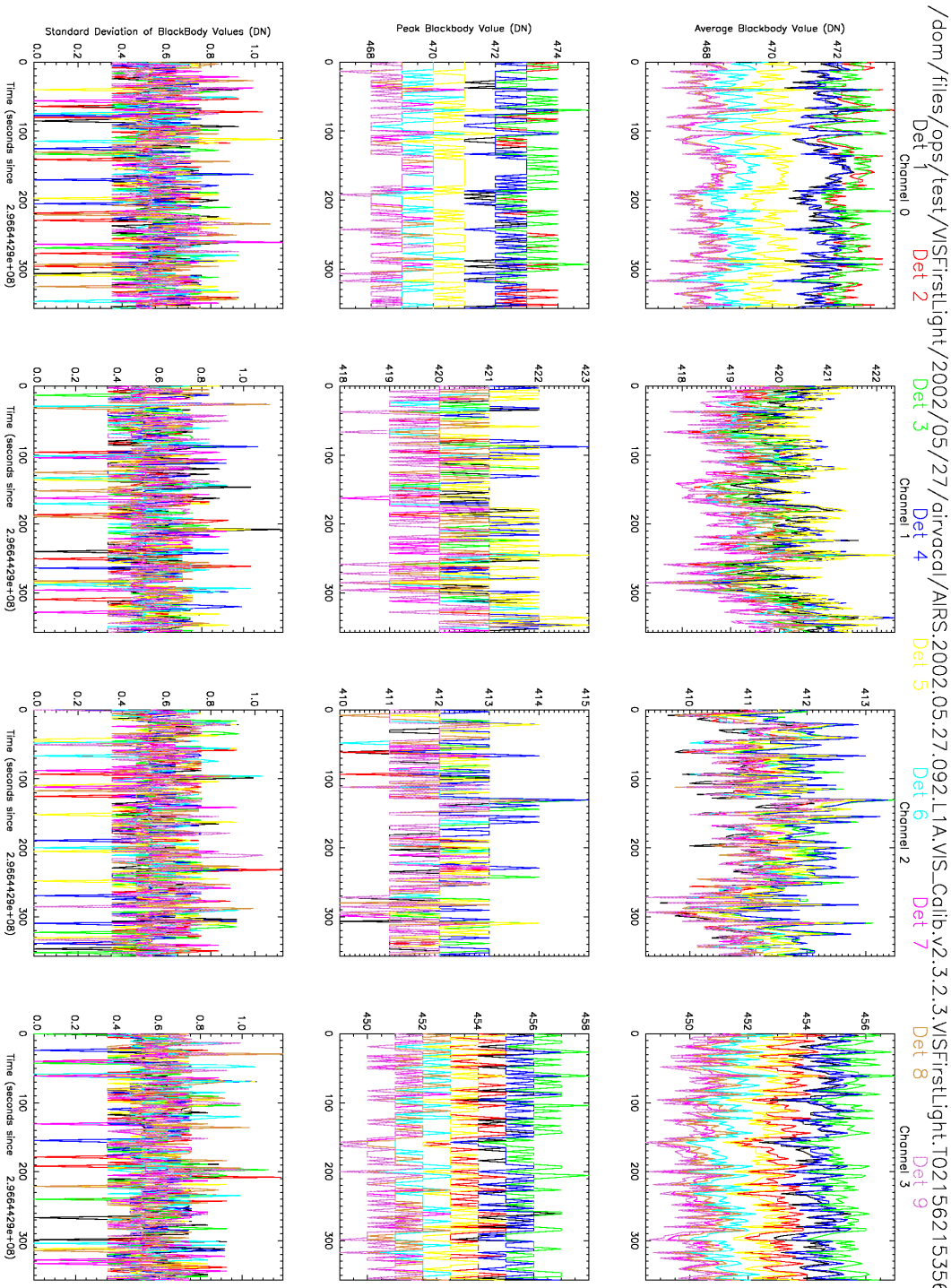


Figure 1: Summary of data collected staring into the blackbody cavity (the Vis/NIR dark current) during Granule 092 of 27 May 2002. The x-axis of each plot is time, in seconds, and covers 6 minutes. Each row plots a different quantity, and each column is for one of the 4 channels. The 9 detectors of each channel are color coded as per the legend at the top of the page. The top row shows the average of the 8 blackbody samples as a function of scanline (time). The middle row gives the peak of the 8 samples. The bottom row shows the standard deviation of the 8 samples within each scanline, which is a useful noise measure of the Vis/NIR system.

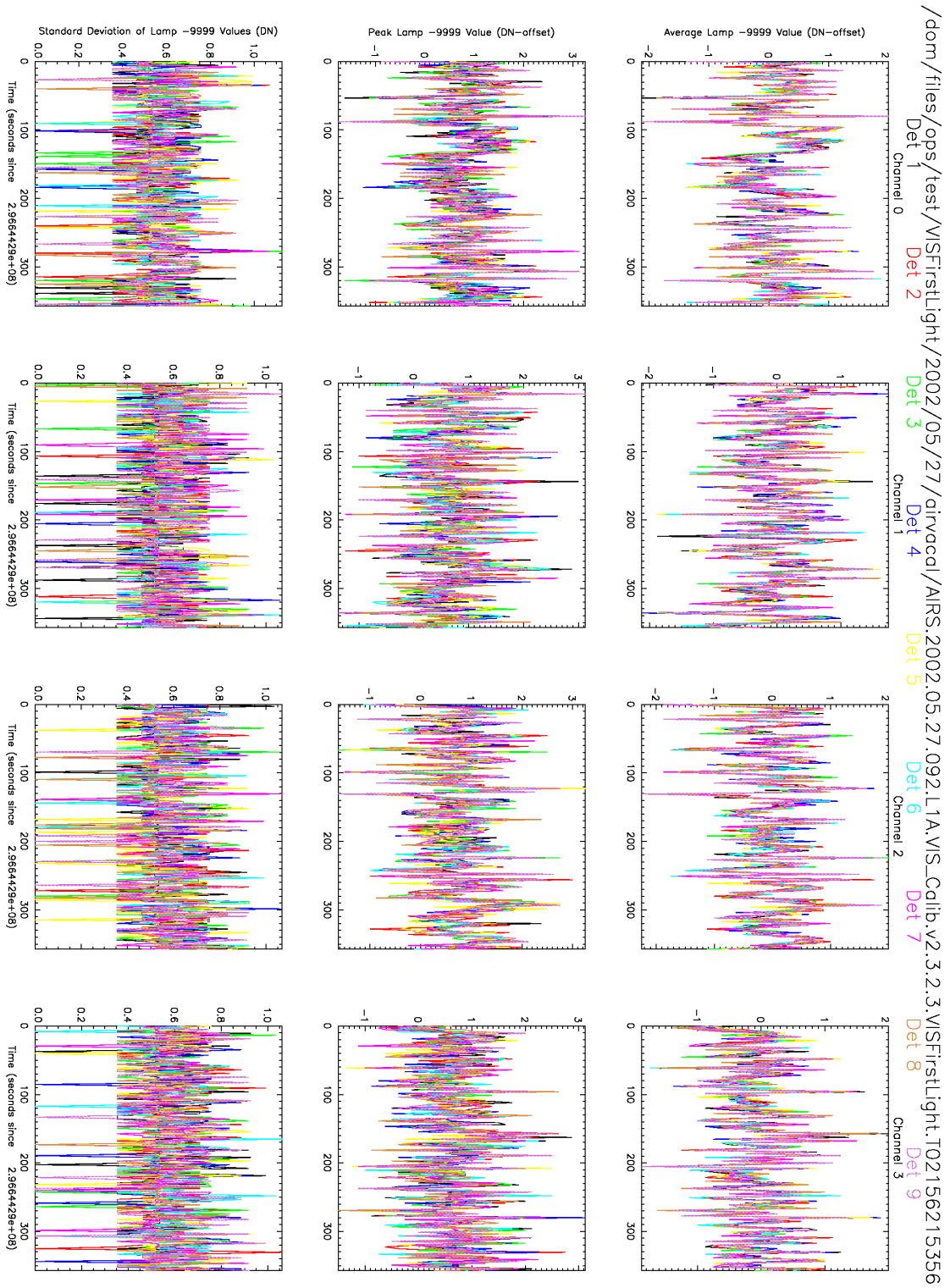


Figure 2: Same as Fig. 1, but showing the data collected while staring into the photometric calibrator assembly. Also, instead of raw counts being plotted, we show DN values with the offset term (the average blackbody signal) subtracted. Since no lamp was on during this granule, these data are another measure of the dark-current and noise levels.

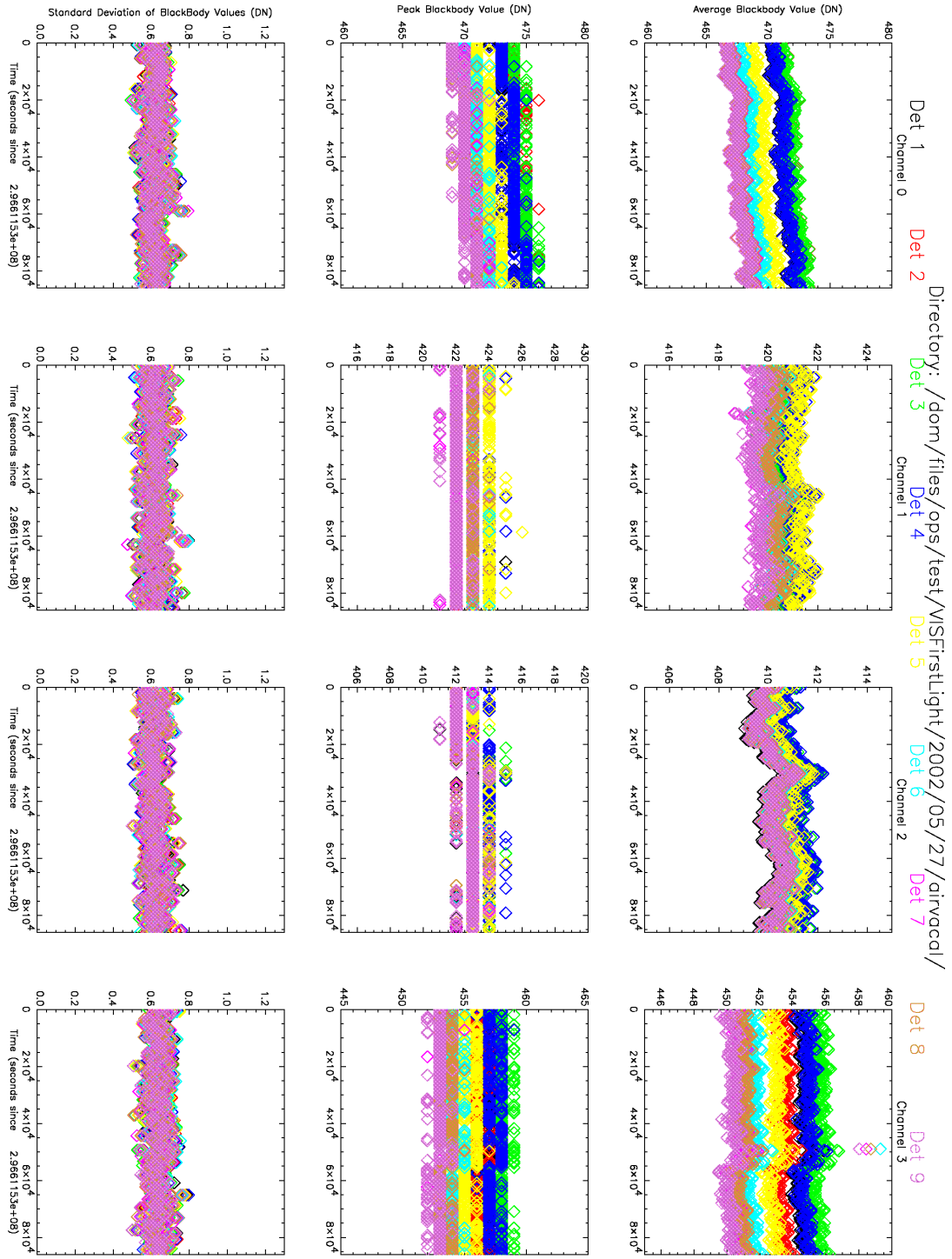


Figure 3: Summary of the blackbody signal observed over all 240 granules of 27 May 2002. Values plotted are similar to those of Fig. 1, but now each symbol is an average of one entire granule. Each column is for one Vis/NIR channel. The x-axis is time, in seconds, and covers 24 hours. The 9 detectors of each channel are color coded as per the legend at the top of the page. The top row shows the average blackbody value in each granule. The middle row gives the peak blackbody value observed in the granule. The bottom row shows the standard deviation of blackbody values within each granule.

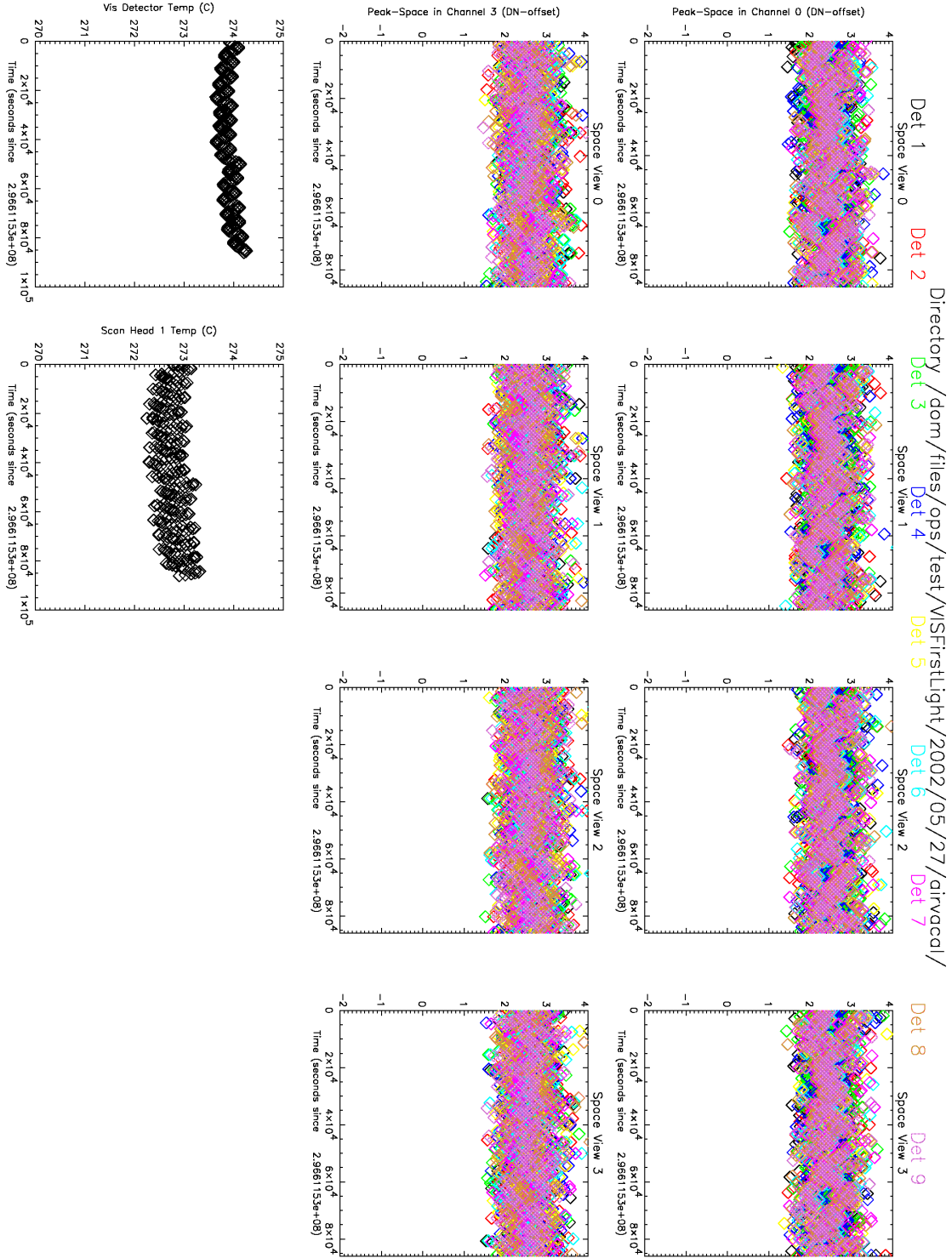


Figure 4: Summary of space-view and engineering temperatures observed over all 240 granules of 27 May 2002. Each symbol is an average of one entire granule. Note that, unlike previous plots, column does not indicate channel. The x-axis is time, in seconds, and covers 24 hours. The top two rows show the peak signal observed in all four space-view ports for channels 0 and 3. The bottom row shows two engineering temperatures as a function of time. Orbital oscillations (roughly 15 per day) are apparent.

Dark Current and Noise Levels

The standard measure of Vis/NIR detector noise used is the standard deviation of the 8 samples obtained while looking into the blackbody cavity. This measurement is made once per scanline (every 8/3 seconds). Figure 1 shows the results for all detectors during one granule. Values are typically about 0.6 data numbers (DN). This is in excellent agreement with pre-launch values. Visual inspection shows no change in noise level between data collected while the scan mirror was parked and while rotating. Figure 1 also shows peak and average DN values observed in each scanline. These values also are an excellent match to pre-launch values. Note that among the 9 pixels in each channel, dark-current response is slightly more uniform within zero-based Channels 1 and 2 than in Channels 0 and 3.

A measure of the extreme short term stability (fraction of a second) of the system is evidenced by Fig. 2, which shows the average signal looking into the photometric calibrator assembly while the lamps are all off. Since the photometric signal is plotted with the dark-current level removed, the fact that the signal is nicely centered on zero shows this stability. The peak and standard deviation of the “lamp” signal are also shown, and it is reassuring that they are very similar to the dark-current values of Fig. 1. Figure 3 shows the longer term (daily) stability of the system. Note that the noise level (the blackbody standard deviation) is stable throughout, while the absolute dark-current level shows variations which are probably due to temperature variations of the detectors (Fig. 4). These temperature effects are removed by the dark-current subtraction process, as evidenced by the lack of temperature-correlated variability in lamp signal (shown in the next section).

An attempt was made to pick out the South Atlantic Anomaly (SAA), where the rms noise and peak levels might be expected to rise due to the charged particle flux. No change is apparent to the eye, as can be seen in Fig. 3, where transits of the SAA occur at times around 0.9, 1.5, 2.1, 5.3, 5.9, and 6.4x10⁴ seconds, corresponding to granules 26, 42, 59, 147, 164, and 180, respectively.

There does appear to be a subtle structure in the blackbody signal. Figure 5 shows that the low-numbered detectors of (zero-based) Channel 2 tend to have a higher value in the last of the 8 blackbody samples. This is true whether lamps are on or off, and the feature does not appear in ground data. Investigation is continuing, but at this time it does not appear to have a significant effect on the Vis/NIR data.

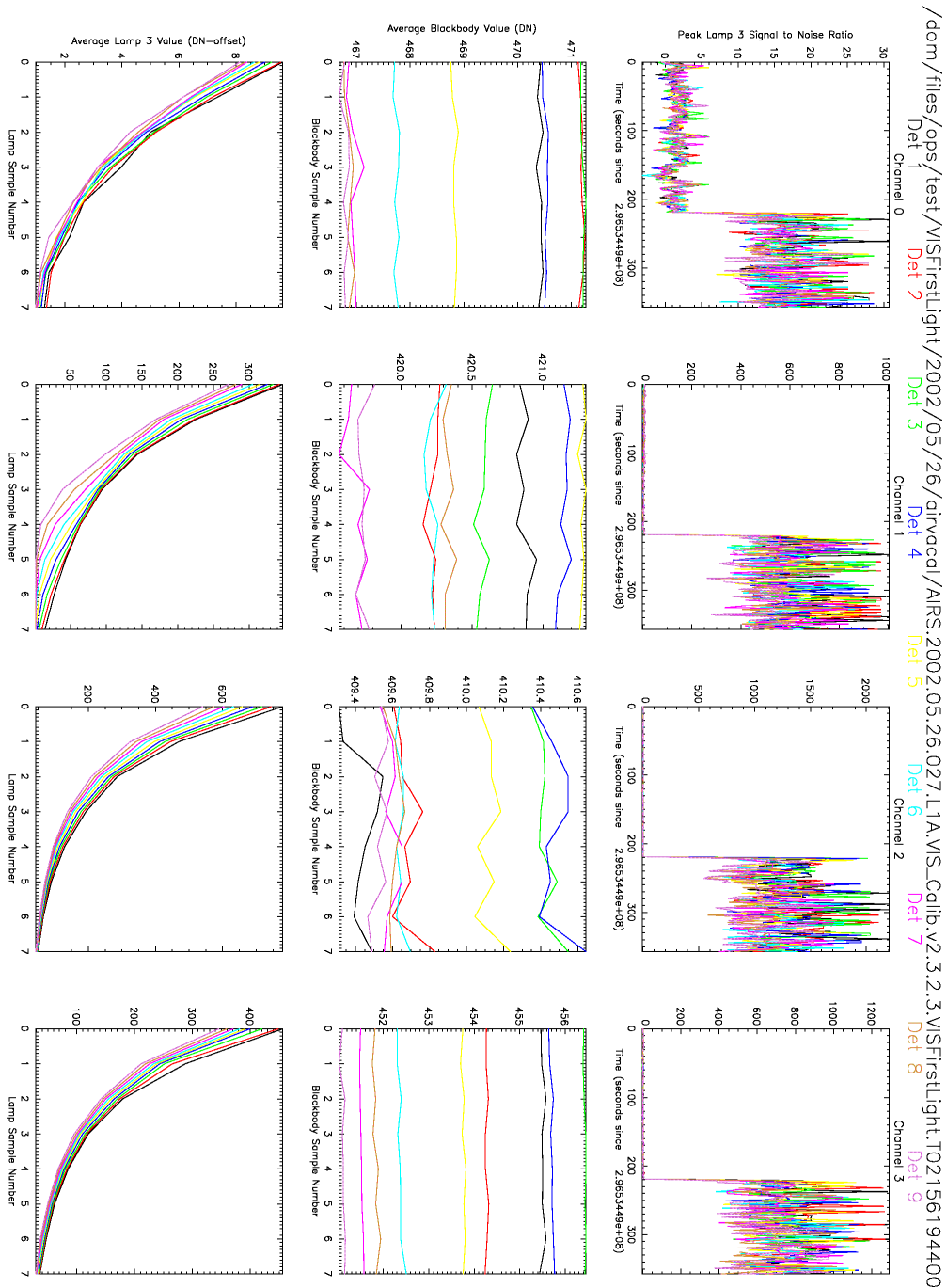


Figure 5: Details of the blackbody signal. The middle row of this chart shows the granule average of each of the 8 blackbody samples collected per scanline. The third column, corresponding to Channel 2, shows that most detectors tend to peak at the 8th sample. The magnitude of this affect is a fraction of a DN, and a formal statistical analysis has not yet been done, but to the eye it appears significant. This feature is seen in all data collect on-orbit, whether a lamp is on or not. The feature does not appear in ground data. The top row shows the lamp signal to noise ratio (peak lamp signal divided by noise), which is not discussed in this memo. The bottom row shows the detailed structure of the lamp signal, averaged over all scanlines of the granule. Compare to Fig. 11a, which shows the detail for one scanline.

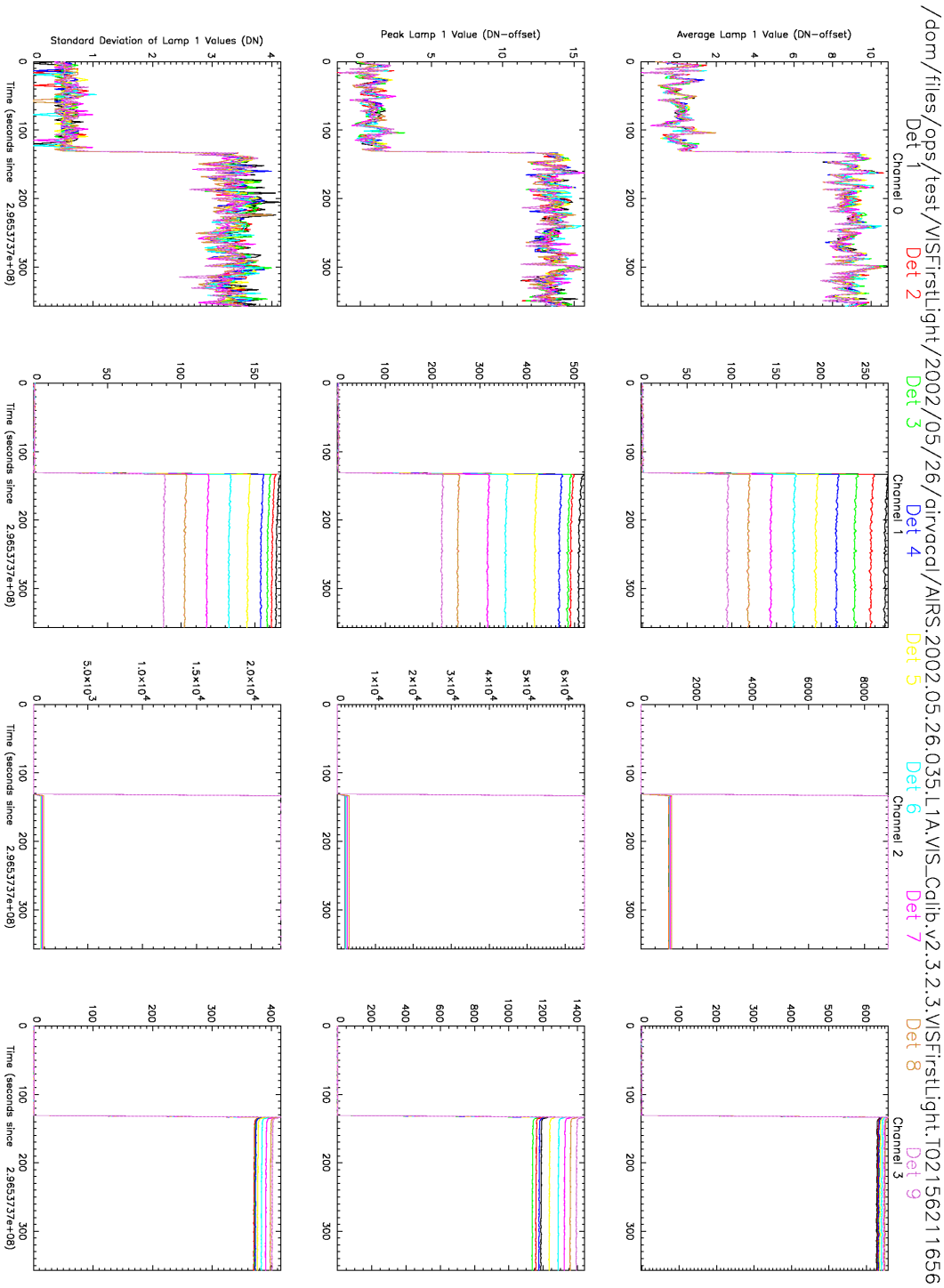


Figure 6: Summary of Lamp 1 performance in Granule 035 of 26 May 2002. As before, the columns indicate the response of each of our 4 channels, and each row plots a different quantity. The x-axis is time. The top row is the average signal (offset subtracted) from the 8 samples in each scanline. The middle row gives the peak value of the 8, as a function of scanline. The bottom row gives the standard deviation of the 8 samples. Note that the lamp was turned on mid-granule, causing a jump in all the curves. Also note that Detector 9 of Channel 2 saturates.

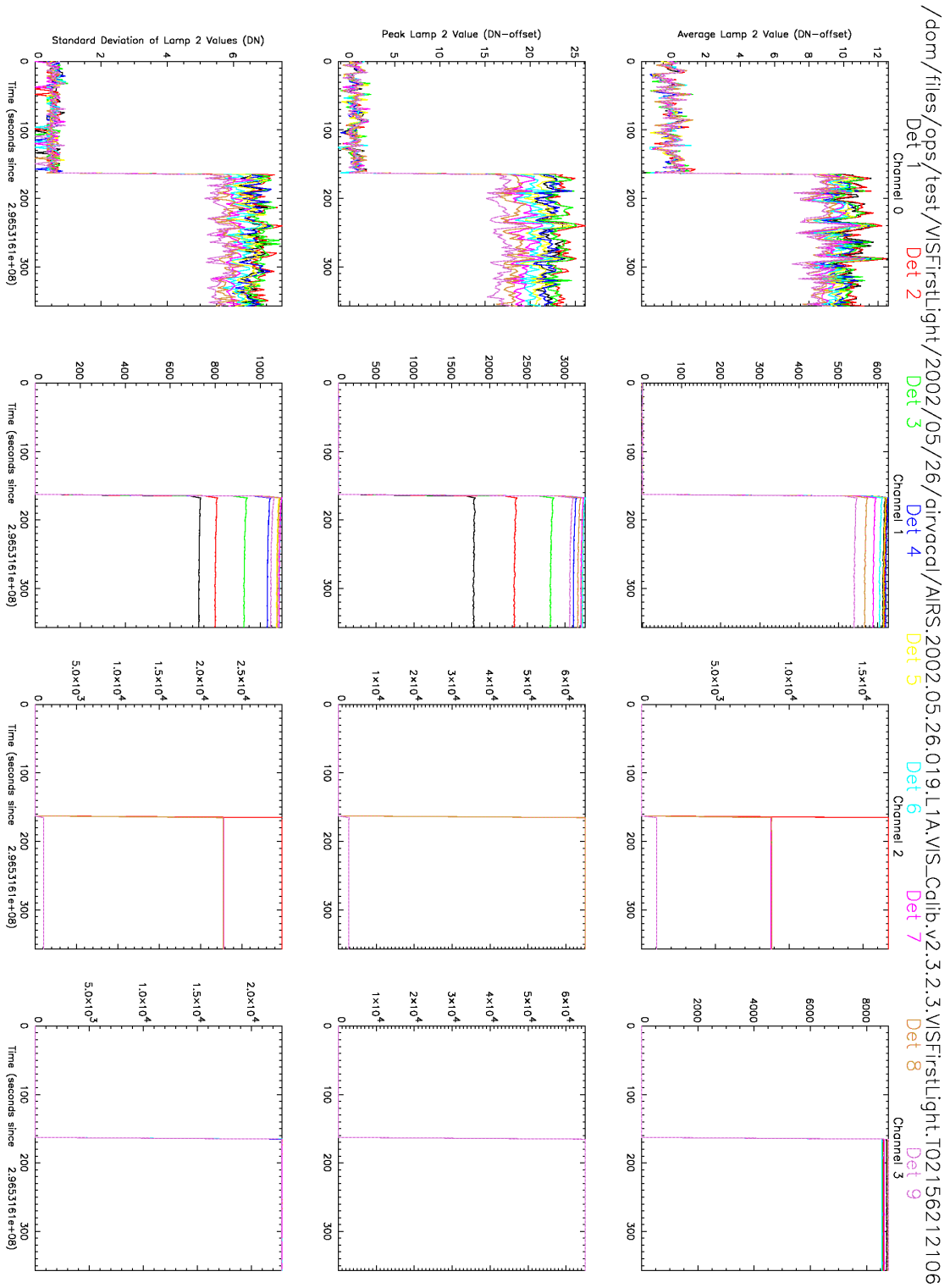


Figure 7: Similar to Fig. 6, except showing Lamp 2 in Granule 019 of 26 May 2002. This lamp saturates detectors in both Channels 2 and 3.

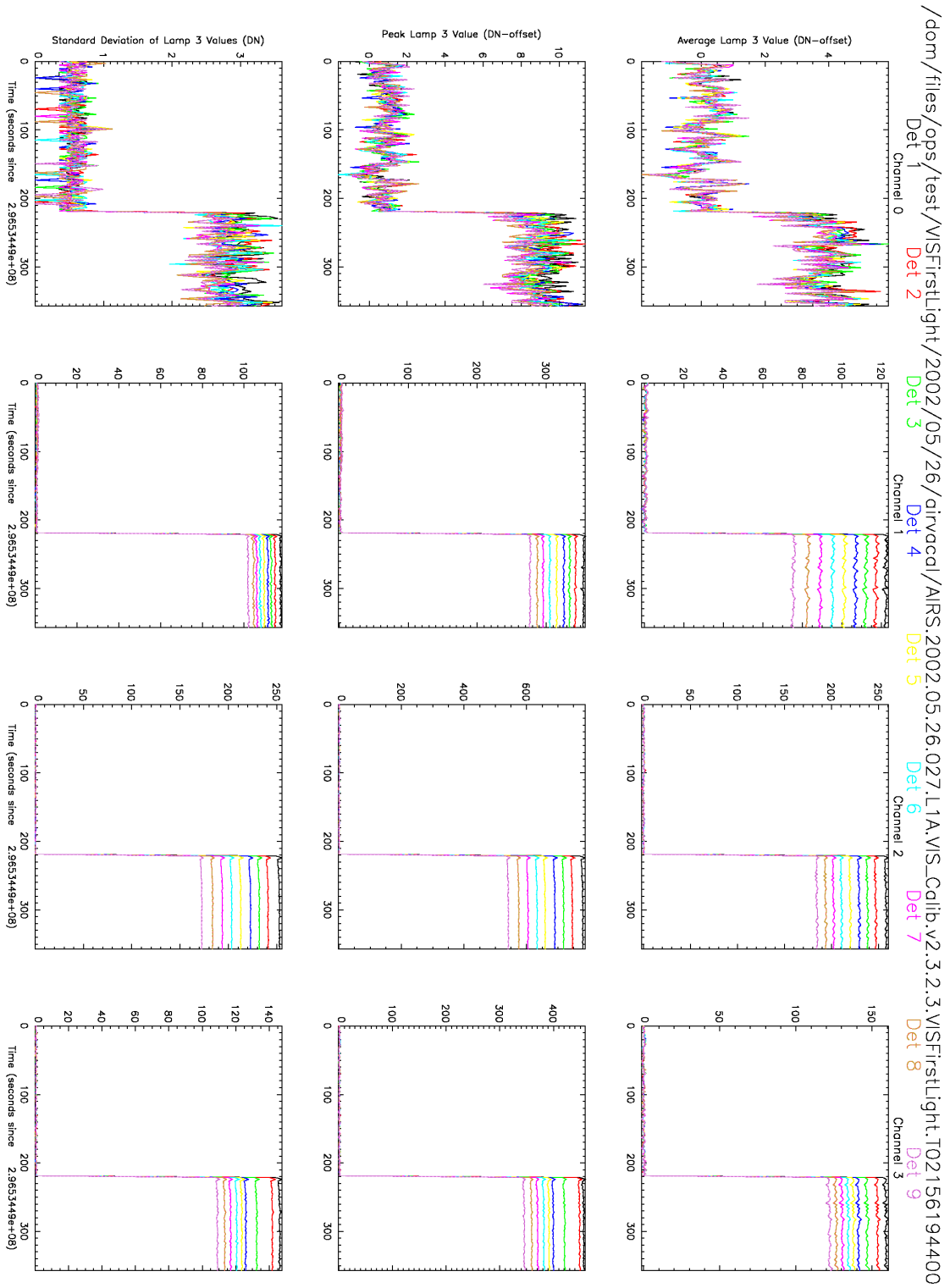


Figure 8: Similar to Fig. 6, except showing Lamp 3 in Granule 027 of 26 May 2002. This is the only lamp that does not saturate any detectors.

Lamp Performance

Each calibration lamp was turned on for 8 minutes during the first day of operation. For the next few days, Lamp 1* was turned on for 8 minutes every 200 minutes. After a few day's hiatus, Lamp 3 is currently set to come on once per day, for 8 minutes. This pattern is expected to continue for several more weeks, at which time lamp operation plans will be reassessed in light of system stability to date.

The average, peak, and standard deviation of lamp signals for each scanline in a granule is shown in Figs. 6 through 8. Stability and noise levels are similar to what has been observed on the ground. Note the turn-on transients, which are discussed in ADF-558 and ADF-559, based on pre-launch data. As per the pre-launch plan, these transient effects are removed from gain calculations by ignoring the first few minutes of lamp data. The detailed turn-on behavior will be investigated at a later date.

While lamp signal levels are similar to pre-launch measurements, they are not identical. Figures 9, 10, and 11 compare the detailed brightness pattern seen from each lamp during ground thermal vacuum testing at TRW and after launch. Signal level differences are apparent for each lamp, though the overall shapes remain the same. The most significant change is that Detector 9** of (zero-based) Channel 2 now saturates when observing Lamp 1 (Fig. 9). This change appears to have occurred on the ground, between the TRW facility and Vandenberg Air Force Base (VAFB), since TV test 511 (conducted at VAFB with Lamp 1 on) shows saturation as in the flight data. Also note that Lamp 2 has always saturated detectors in Channels 2 and 3 (Fig. 10), and this behavior has not changed.

At this time we cannot say whether the lamp signal changes are due to a change in lamp performance, detector response, or the physical alignment of elements in the system (photocalibrator assembly, detector arrays, scan mirror, or scan profile). During ground testing, the detailed lamp response was also seen to change between testing phases (see, for example, the 14 September 1999 Lockheed Martin internal memo from Gary Tarnowski to Ken Overoye). Most changes on the ground were attributed to slight alignment differences due to changes in the scan profile, physical readjustment of the photocalibrator assembly, or, in at least one case, vibration testing. For Vis/NIR purposes, the changes observed to date are irrelevant, as long as the system is now stable. The saturation of some detectors by some lamps is a nuisance, but is unlikely to affect overall calibration quality. This situation will be monitored over the coming months.

* By convention, the three calibration lamps are designated 1, 2, and 3, even when working in a zero-based environment.

** As with the lamps, detectors are always numbered 1 through 9, even in zero-based discussions. Note, however, that detector numbering changed as of approximately 6 June 2002, with version 2.3.2 of the PGE. Prior to this version, Detector 1 is the farthest along-track. From v2.3.2 onward, Detector 9 is farthest along track. (This change was implemented to make data products more consistent internally, and consistent with standard imaging practice.)

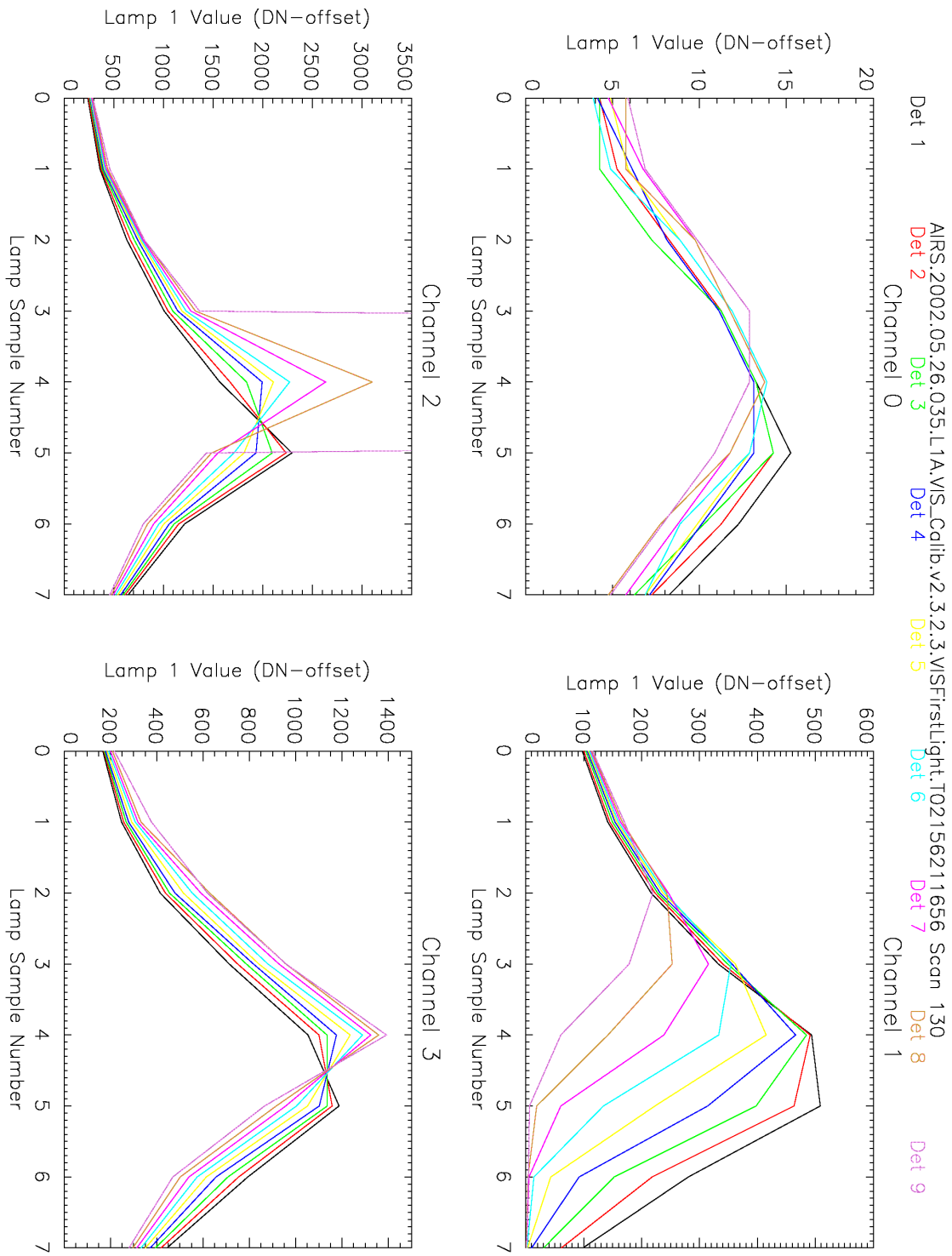


Figure 9a: Details of the signal from Lamp 1 on orbit. These plots show the 8 samples (x-axis) made by each of the 9 detectors in each of our 4 channels. Scanline 130 of Granule 035 of 26 May 2002 is shown. Compare to Fig. 9b, which shows data collected pre-launch.

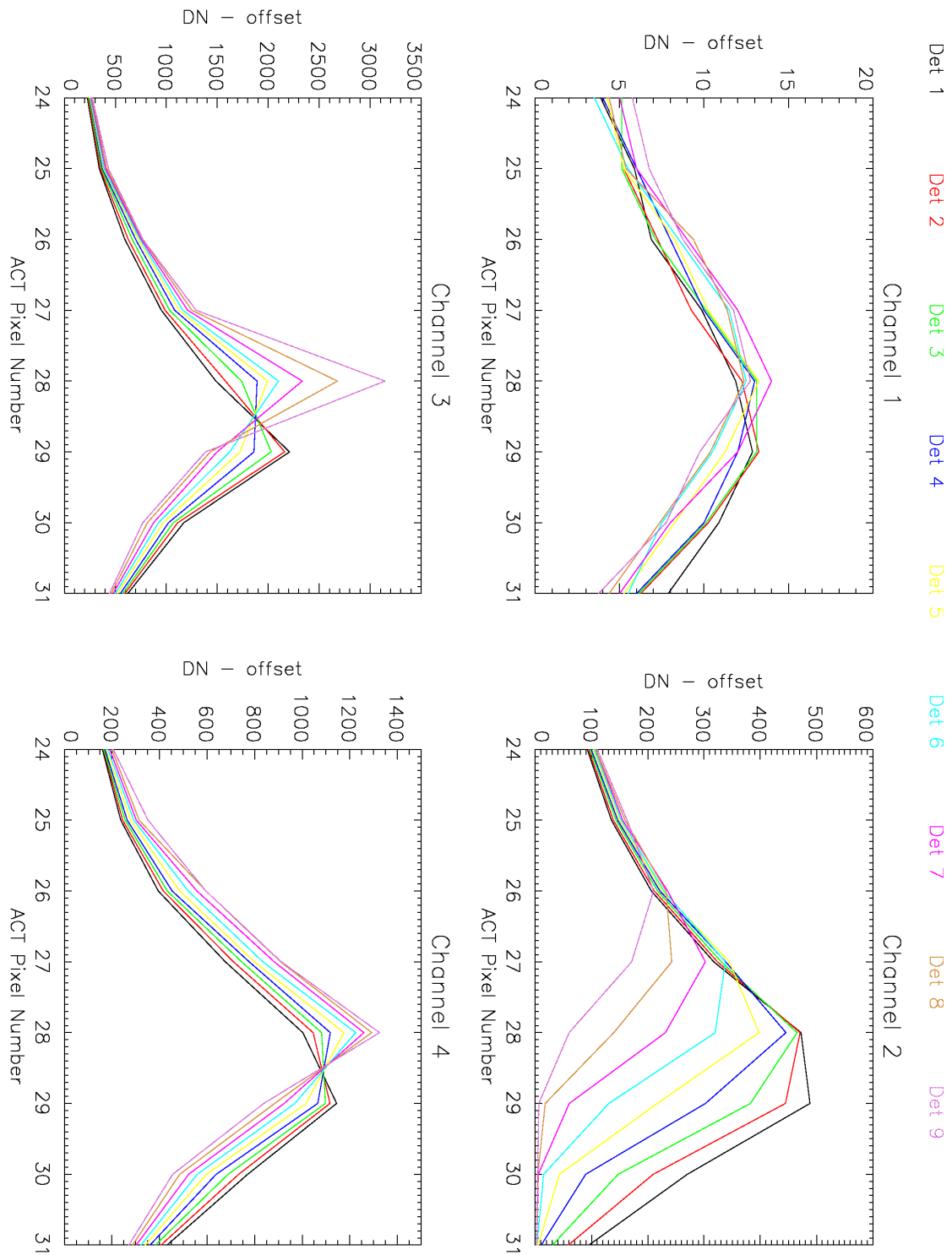


Figure 9b: Details of the signal from Lamp 1 during ground test. These plots show the 8 samples (x-axis) made by each of the 9 detectors in each of our 4 channels. Scanline 100 of TV test 146 is shown. Compare to Fig. 9a, which shows data collected on orbit.

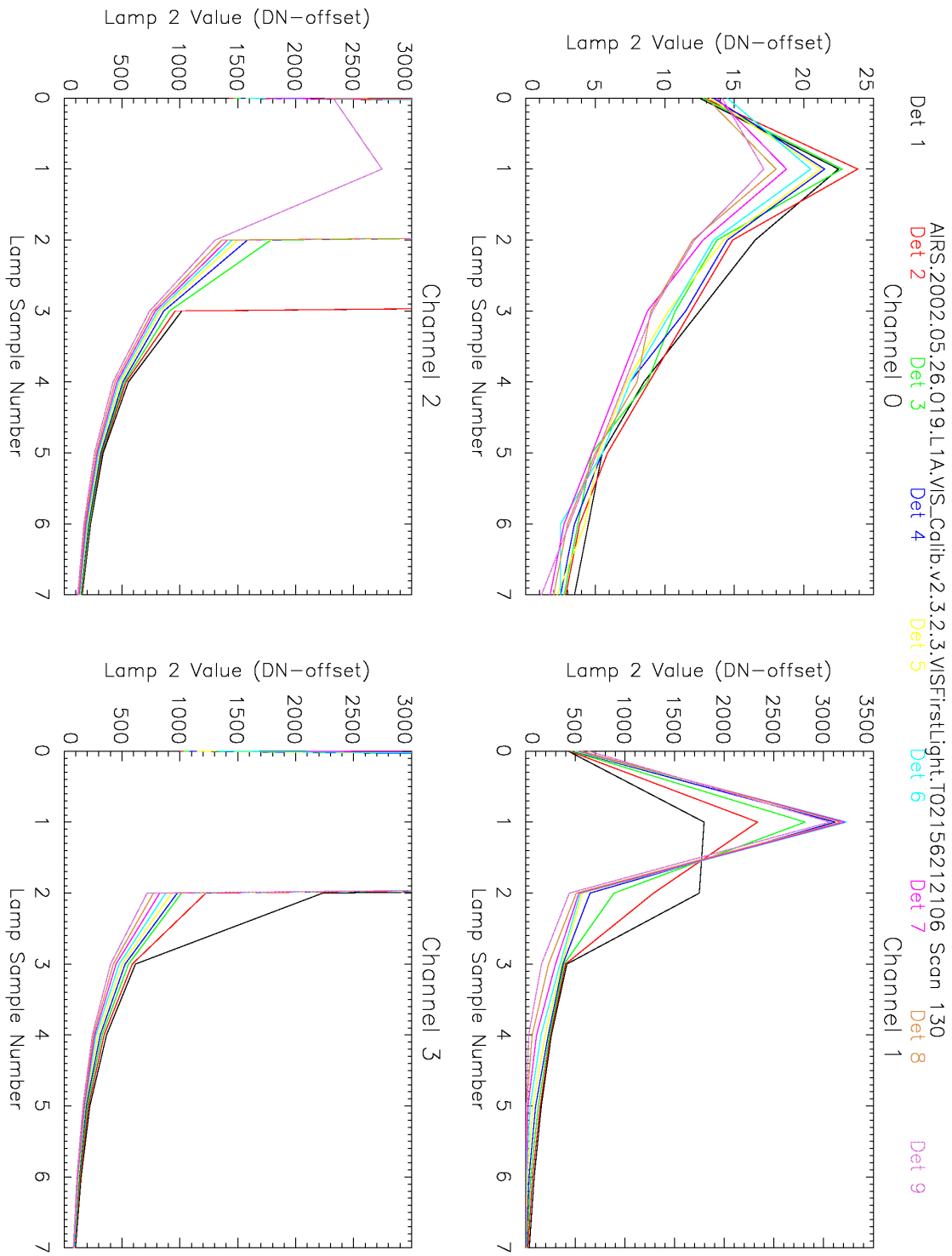


Figure 10a: Details of the signal from Lamp 2 on orbit. These plots show the 8 samples (x-axis) made by each of the 9 detectors in each of our 4 channels. Scanline 130 of Granule 019 of 26 May 2002 is shown. Compare to Fig. 10b, which shows data collected pre-launch.

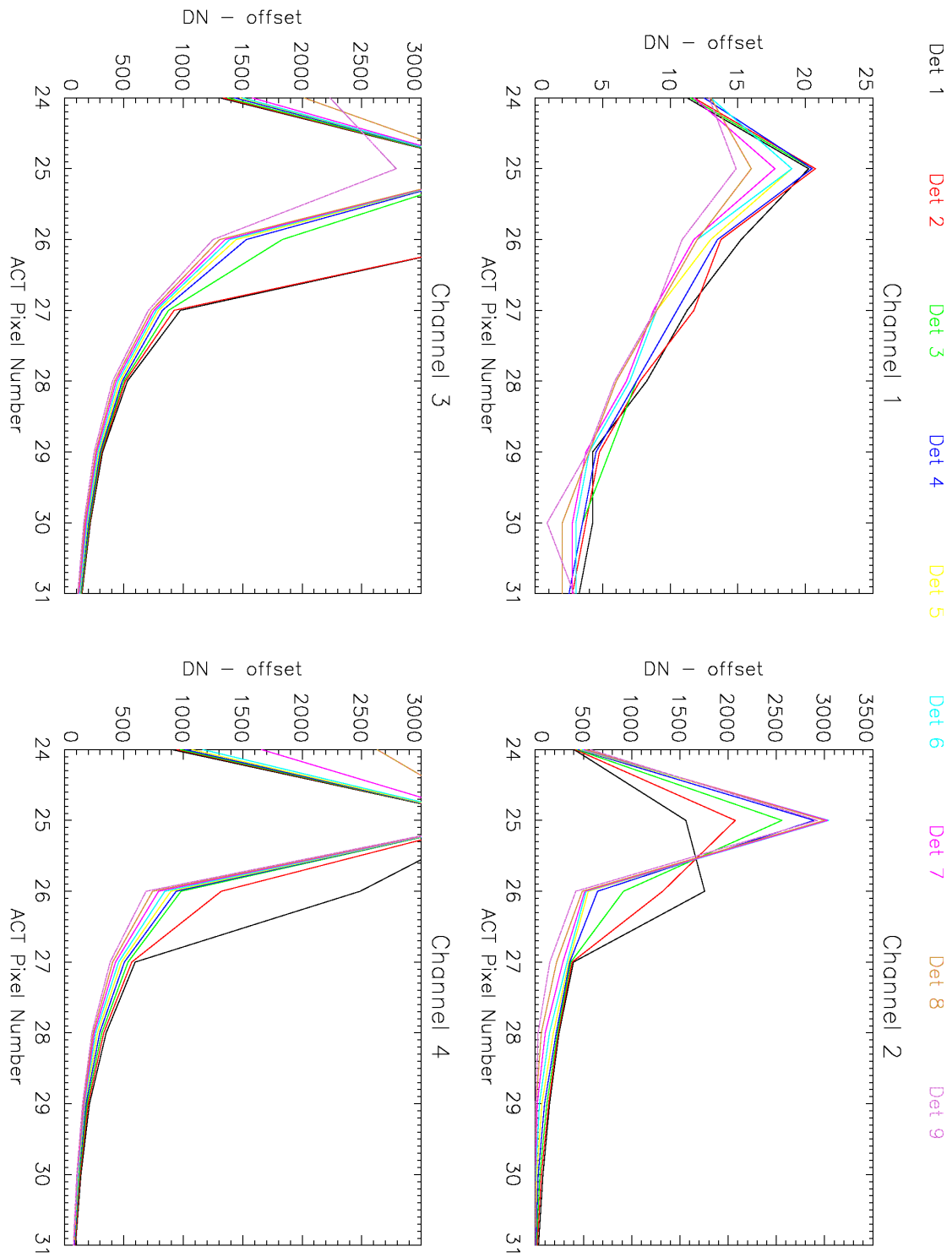


Figure 10b: Details of the signal from Lamp 2 during ground test. These plots show the 8 samples (x-axis) made by each of the 9 detectors in each of our 4 channels. Scanline 100 of TV test 147 is shown. Compare to Fig. 10a, which shows data collected on orbit.

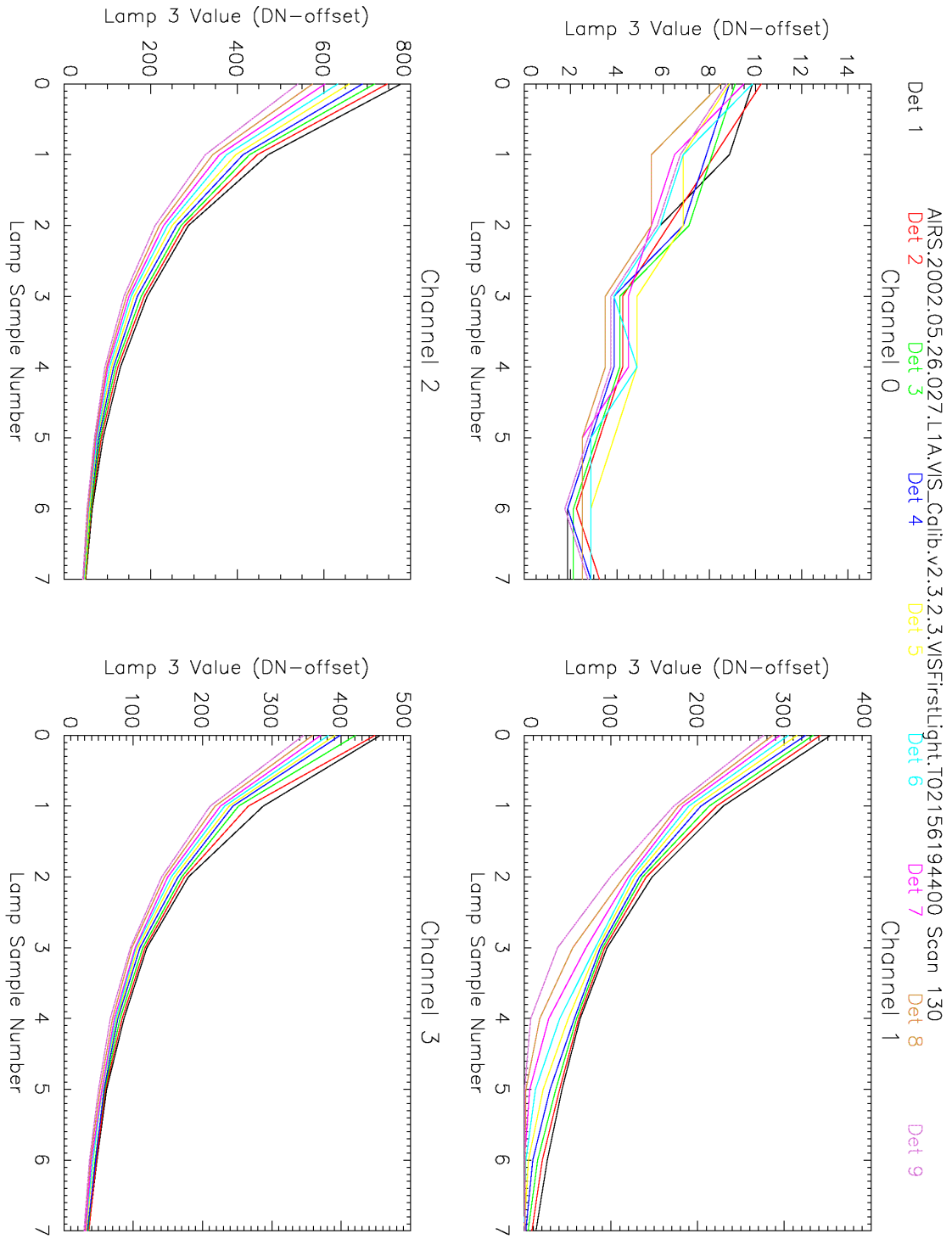


Figure 11a: Details of the signal from Lamp 3 on orbit. These plots show the 8 samples (x-axis) made by each of the 9 detectors in each of our 4 channels. Scanline 130 of Granule 027 of 26 May 2002 is shown. Compare to Fig. 11b, which shows data collected pre-launch.

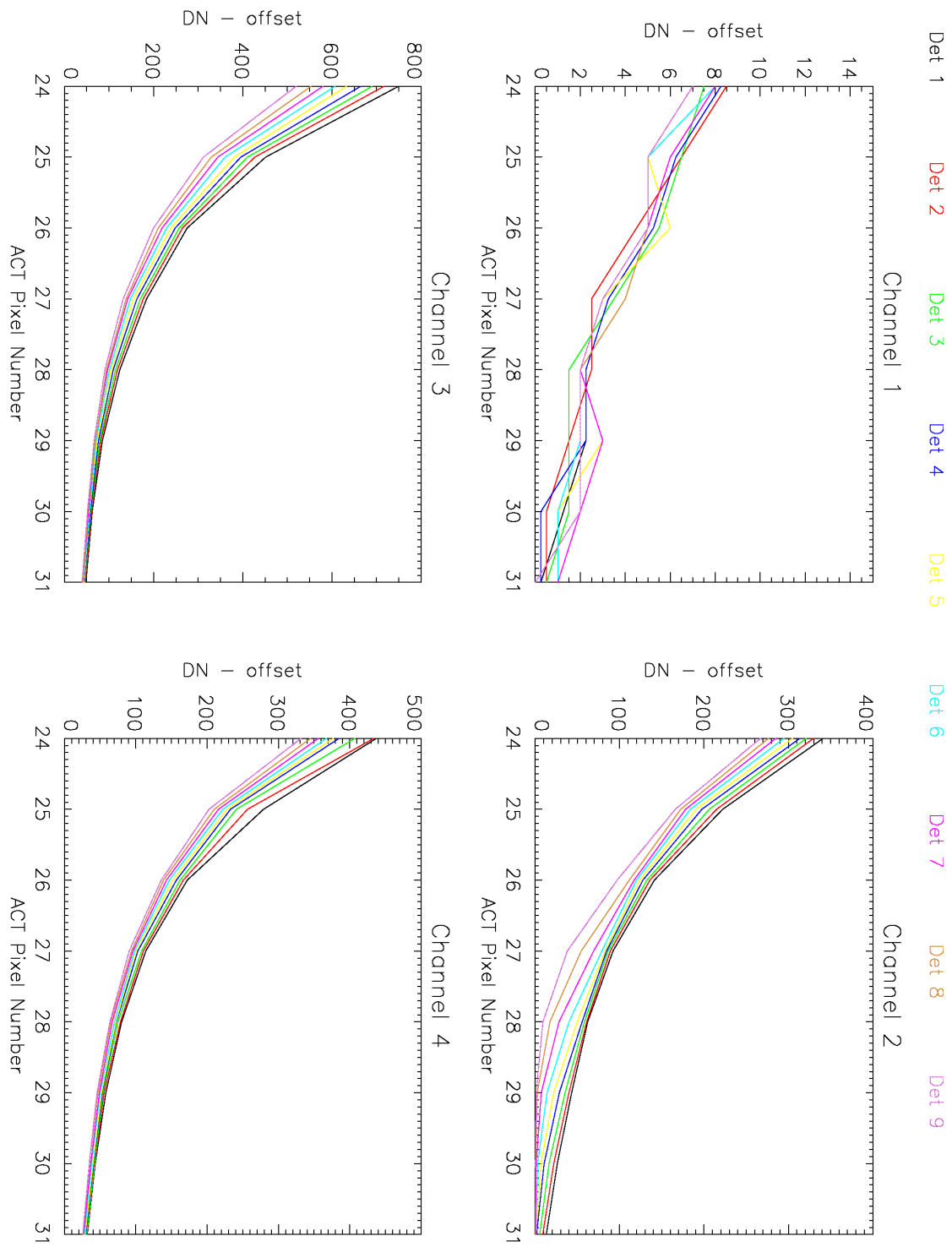


Figure 11b: Details of the signal from Lamp 3 during ground test. These plots show the 8 samples (x-axis) made by each of the 9 detectors in each of our 4 channels. Scanline 100 of TV test 149 is shown. Compare to Fig. 11a, which shows data collected on orbit.

Co-Registration

Initial testing of the co-registration of the four Vis/NIR channels is done by eye. (A more quantitative analysis will be performed after bringing the cloud detection algorithm on-line.) In color composite images, such as shown in Fig. 12, co-registration errors would show up as systematic colored “ghosts” around features. Inspection of numerous images, particularly cloud edges over ocean (in which ghosts would be easiest to spot) show no evidence of mis-registration. We also induced deliberate spatial offsets among the channels to see if the resulting images looked better. In every case, image quality dramatically decreased with induced offset (an example is also shown in Fig. 12). We therefore conclude that the channels are aligned to at least the instrument resolution, which is 0.185 degrees, or about 2~km for the current orbit.

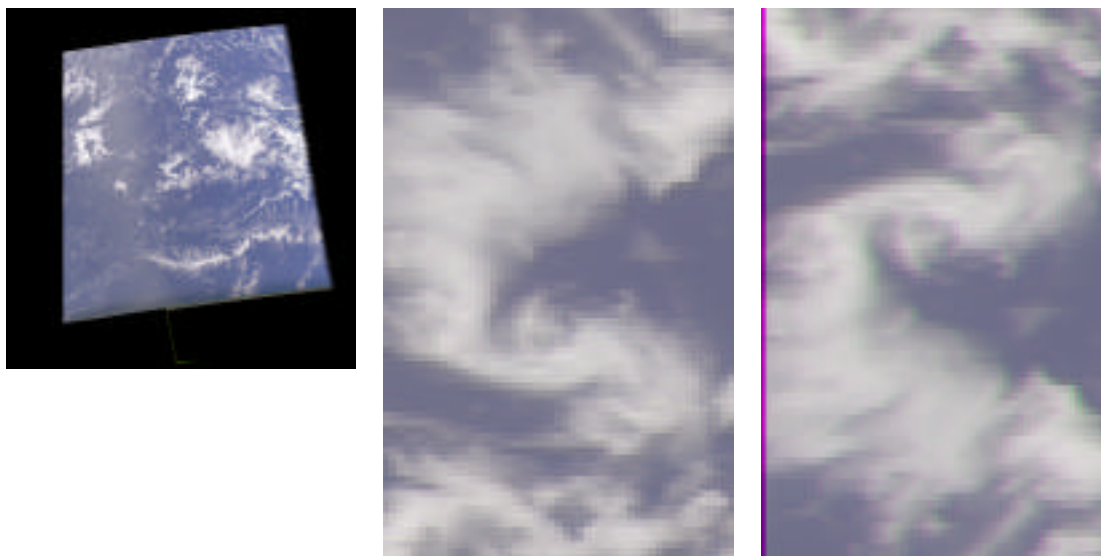


Figure 12: Co-registration test. These images are AIRS “first light” data, Granule 011 of 26 May 2002, collected over the equatorial Pacific southwest of Hawaii. On the left is the entire granule, with Vis/NIR zero-based Channels 2, 1, and 0 plotted as red, green, and blue, respectively. Note the affect of sunglint along the left side of the image. The middle panel shows a blow-up of the central region of the granule. The relatively pure white and blue colors at cloud/ocean boundaries are an indication that the three channels are co-located. Similar images have been made incorporating Channel 3. The right panel shows a nearby region, with a deliberate offset in the green channel applied. The offset is about 75% of a pixel to the right, and we clearly see a green tint on the right side of clouds, and a purple one on the left.

Geolocation

As with co-registration, initial validation of the absolute geolocation of Vis/NIR products is done by eye. We use MISR-Terra images, collected by their nadir camera, as our absolute reference. These MISR images have 275 meter resolution, and their geolocation (based on USGS topographic maps and specially processed LANDSAT images) is believed to be accurate to 100 meters or better, avoiding systematic errors recently found in standard references such as the WDB2 coastline map (personal communications with Jim Knighton and Dave Gregorich).

Validation is done by linking geolocated Vis/NIR and MISR radiance maps within the Vendaval software tool at the TLSCF. Viewing both images at high resolution, so that the pixelation of each image is clear (Fig. 13), one can run a cursor along features in one image, and a marker will move along the corresponding location in the other image. We have done this for coastlines and rivers at nadir and near the western edge of the swath, and in no case is a mismatch observed. (Vis/NIR granule 117 of 27 May 2002 has been compared to a MISR image along Path 044, Blocks 58 to 63, collected on 30 September 2001, and Vis/NIR granule 215 of 27 May 2002 has been compared to MISR path 185, Blocks 58 to 66, of 24 May 2002.) We therefore conclude that the geolocation in Vis/NIR products (at least from software versions 2.3.1.3 and 2.3.2.3) is accurate to one Vis/NIR pixel, corresponding to 0.185 degrees or ~2 km on the ground at nadir. This validates not only the AIRS PGE to this level, but also the spacecraft attitude and location information received from the DAAC approximately 24 hours after data collection. Area matching software will be run in the future to provide a more accurate, numerical estimate of geolocation accuracy.

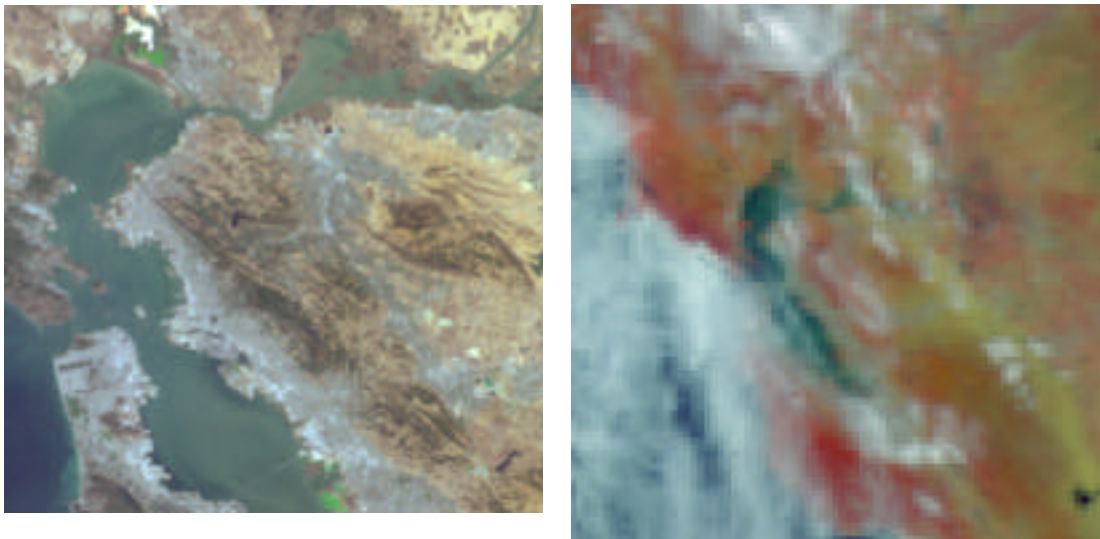


Figure 13: Geolocation test. On the left is a geolocated MISR nadir camera image of the San Francisco Bay area, taken on 30 September 2001. The resolution is about 275 meters. On the right is geolocated Vis/NIR data over the same region, collected on 27 May 2002. These data are from the edge of the swath, so the instrument resolution is only about 3.5 km, and the image shown has been further spatially degraded by making a cylindrical map projection. When validating geolocation, a non-projected image is used to maximize spatial resolution. As discussed in the text, detailed comparison of images such as these allow us to say the Vis/NIR data is properly geolocated.